

A General Route to Robust Nacre-Like Graphene Oxide Films

Zhibing Tan,^{†,‡} Miao Zhang,[‡] Chun Li,^{*,‡} Shiyong Yu,^{*,†} and Gaoquan Shi^{*,‡}

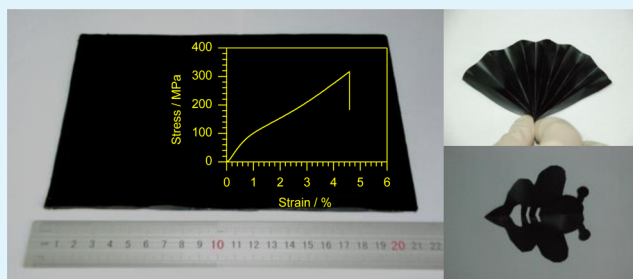
[†]School of Chemistry and Chemical Engineering, Inner Mongolia University, Hohhot 010021, China

[‡]Department of Chemistry, Tsinghua University, Beijing 100084, China

S Supporting Information

ABSTRACT: Artificial nacre-like composite films of graphene oxide (GO) with a variety of commercially available water-soluble polymers were fabricated by a gel–film transformation (GFT) technique. The blending of a polymer into the aqueous dispersion of GO can modulate the interaction between GO sheets. Typically, the attraction force between polymer and GO sheets overcomes the dominant hydration and electrostatic repulsive forces between GO sheets, promoting the gelation of GO. Cast drying the resultant GO hydrogel containing small amounts of polymer (1–20 wt % relative to GO depending on the intrinsic structures of polymers) generates layered GO composite films with tensile strengths over 200 MPa and failure strains larger than 3.0%, which are higher than those of natural nacre and most nacre-like GO films. These results indicate that GO/polymer composite hydrogels are excellent precursors for nacre-like GO films and that the GFT approach is a general route toward the large-scale fabrication of nacre-like GO films with unique combinations of high strength and high toughness.

KEYWORDS: graphene oxide, gelation, artificial nacre, hierarchical structure, mechanical properties



1. INTRODUCTION

Artificial nacre-like films have attracted increasing interest because of their light weight, high strength, stiffness, and toughness.^{1–5} Graphene oxide (GO) sheets are promising building blocks for these materials because of their inherent 2D structures, superior mechanical properties, excellent solution processability, and ample oxygenated moieties for enhancing interfacial interactions between the adjacent GO sheets.⁴ During the past decade, various strategies have been developed to prepare nacre-like GO composites,⁴ including vacuum-assisted filtration,^{6–17} layer-by-layer assembly,^{12,18} evaporation-induced self-assembly,¹⁹ electrospray deposition,²⁰ and wet-spinning assembly.²¹ Among them, vacuum-assisted filtration is the most widely used method to prepare GO films with orderly laminated architectures and high mechanical performance.^{4,6–17} However, this method usually produces small pieces of films because of the limitation of the filtration apparatus. Relatively large GO films can be generated by evaporation-induced self-assembly and electrospray deposition at the expense of their mechanical performance.^{20,21} Accordingly, it still remains a great challenge to develop a general strategy to produce large-area, robust nacre-like GO films with the integration of high tensile strength, large failure strain, and excellent toughness.

Recently, we reported a facile gel–film transformation (GFT) method to prepare robust nacre-like GO composite films by cast drying GO hydrogels with small amounts of polymers.^{22,23} These examples indicate that the GO/polymer hydrogels are good precursors for the large-scale fabrication of robust nacre-like GO composite films. However, the GFT

method has not yet been studied extensively, and its wide applicability has also not been confirmed. Here, we report a systematic study on the GFT method that examines a variety of commercially available water-soluble polymers as gel promoters. The influences of polymer and GO structures on the mechanical properties of nacre-like GO composite films were also evaluated. It was found that small quantities of polymers (1–15 wt % relative to GO depending on the polymer intrinsic structures) can efficiently induce the self-assembly of GO sheets into hydrogels through hydrogen bonding, electrostatic interaction, hydrophobic effect, and/or their synergistic interactions.^{24–27} The obtained GO/polymer composite hydrogels can be transformed to films with hierarchically layered structures by evaporation assembly under ambient conditions. These nacre-like GO composite films showed high tensile strengths over 200 MPa irrespective of the structures and molar masses of the polymers. These results demonstrate that the GFT method is a general approach to prepare nacre-like GO films with high mechanical performances. With the rational selection of GO sheets, the tensile strength, failure strain, and toughness of the GO composites films with 4 wt % chitosan can reach as high as 309 ± 21 MPa, $5.22 \pm 0.43\%$, and 8.26 ± 0.68 MJ m⁻³, respectively.

Received: May 12, 2015

Accepted: June 26, 2015

Published: June 26, 2015

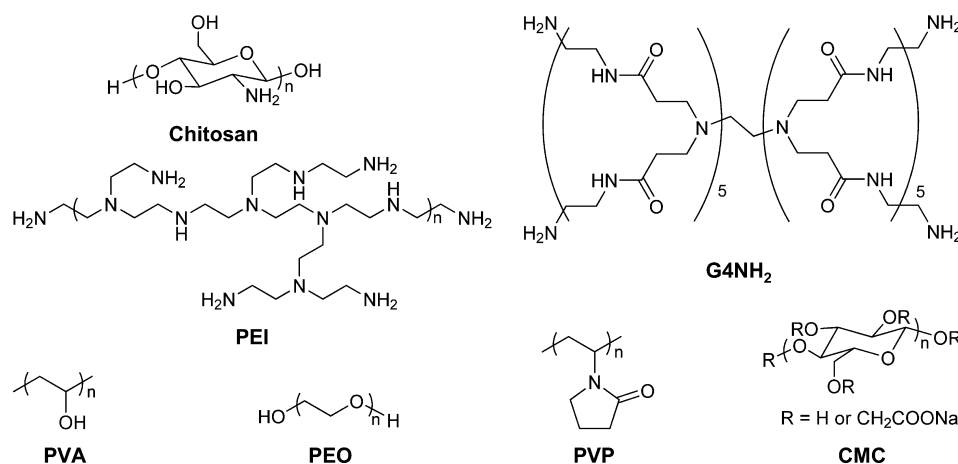


Figure 1. Chemical structures of the polymer promoters for preparing GO composite hydrogels.

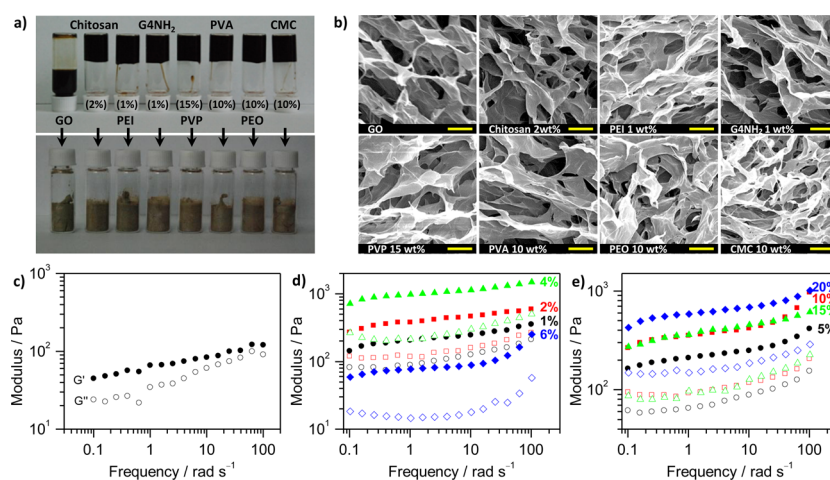


Figure 2. (a) Photographs of a 5 mg mL⁻¹ GO dispersion and its composite hydrogels with different polymer promoters (top) and the corresponding lyophilized samples (bottom). The percentages in parentheses represent the weight ratios of the polymers to GO sheets. (b) Typical SEM images of the lyophilized 5 mg mL⁻¹ GO dispersion and GO composite hydrogels with the compositions as indicated; scale bar = 10 μm. (c–e) Dynamic rheological behaviors of 5 mg mL⁻¹ of (c) aqueous GO dispersion and GO hydrogels containing different amount of (d) chitosan or (e) PVA with the weight ratio relative to GO as indicated. Solid symbols stand for storage modulus (G'), whereas open ones stand for loss modulus (G'').

2. EXPERIMENTAL SECTION

2.1. Materials. Graphite power (325 mesh, Qingdao Huatai Lubricant Sealing S&T Co., Ltd., China), chitosan (50–100 mPa·s, 0.5% in 0.5% acetic acid at 20 °C, Tokyo Chemical Industry Co., Ltd.), polyethylenimine (PEI, branched, $M_w = 70\,000$, Alfa Aesar), fourth-generation amine-terminated poly(amido amine) dendrimer (G4NH₂, 10 wt % methanol solution, $M_w = 14\,215$, Sigma-Aldrich), poly(vinyl alcohol) (PVA, DP = 1750 ± 50, Sinopharm Chemical Reagents Co., Ltd.), polyvinylpyrrolidone (PVP, $M_w = 58\,000$, Sigma-Aldrich), poly(ethylene oxide) (PEO, $M_w = 1\,000\,000$, Alfa Aesar), and sodium carboxymethylcellulose (CMC, 800–1200 cPa·s, Tianjin Jinke Chemical, China) were used as received without further purification.

2.2. Synthesis of GO. GO was prepared by the modified Hummers' method.²⁸ Briefly, graphite powder (3.0 g) and concentrated sulfuric acid (70 mL) were added to a 2 L flask in an ice bath under mechanical stirring (300 rpm), followed by slow addition of potassium permanganate (9.0 g) in small portions to keep the temperature of the reaction mixture lower than 20 °C. The reaction mixture was then warmed up to 40 °C with stirring (300 rpm) for about 30 min. Subsequently, 150 mL of water was added into the mixture, and the obtained dispersion was stirred for 15 min at 95 °C. Finally, an additional 500 mL of water and 15 mL of H₂O₂ (30% aqueous solution) were added to terminate the reaction. The obtained dispersion was filtered and washed with 1:10 HCl aqueous solution

(500 mL) followed by ample water to remove metal ions and residual acid, respectively. The resultant solid was then dispersed in 800 mL of distilled water under vigorous agitation to make an aqueous GO suspension. The obtained GO was further purified by dialysis (molecular weight cut off = 8000–14 000 Da) for 2 weeks to remove trace amounts of acid and metal species. After stirring for 24 h, the resultant GO dispersion was submitted to centrifugation twice at 4000 rpm for 40 min each to remove unexfoliated graphite oxide particles. The final aqueous GO suspension was centrifuged at 8000 rpm for 1 h to remove the ultrasmall GO sheets to some extent. GO' sheets with the larger mean lateral sizes were prepared by the same procedure described above except for lowering the oxidation temperature to 30 °C with a longer oxidation time of 2 h.

2.3. Preparation of the GO Composite Films. Aqueous GO stock dispersion (7.5 mg mL⁻¹) was mixed with a certain amount of polymer solutions with the given concentrations, followed by vigorous stirring for several minutes using a vortex mixer to give 5 mg mL⁻¹ of GO composite dispersions or hydrogels depending on the amount of polymers added (0.5–20 wt % relative to GO). The GO composite films with thickness of 10–12 μm were prepared by cast drying the resultant GO dispersions and hydrogels at room temperature (25 °C, humidity ≈ 50%), which typically takes 48 h. The reduced GO' films containing 4 wt % chitosan were obtained by chemical reduction of GO' films with HI solution (57 wt %) at room temperature for 12 h,

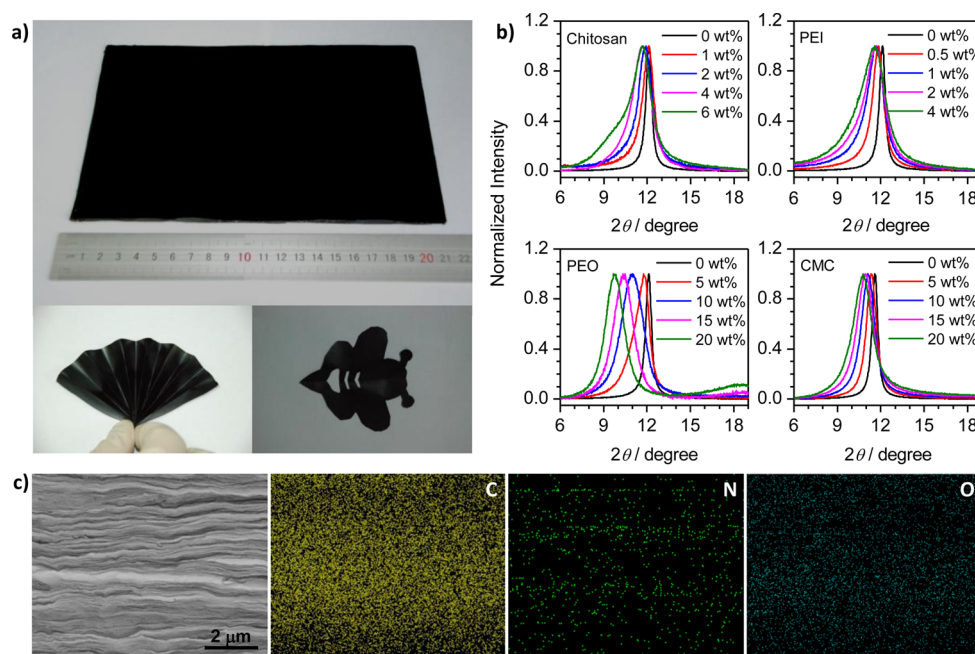


Figure 3. (a) Photographs of GO films containing 2 wt % chitosan (top) and the films with different shapes processed by origami and paper-cutting (bottom). (b) Typical XRD patterns of the GO composite films containing different amounts of polymers as indicated. (c) SEM image of the fractured cross section of GO film with 4 wt % chitosan and the corresponding EDS mappings of C, N, and O elements as indicated.

followed by washing with ample water and drying at room temperature. The control GO/PEO (10 wt %) films with thickness comparable to those prepared by GFT were fabricated by vacuum-assisted filtration of GO dispersion (1 mg mL^{-1}) containing 10 wt % PEO through a poly(tetrafluoro ethylene) (PTFE) membrane (47 mm diameter, $0.22 \text{ } \mu\text{m}$ pore size).

2.4. Characterizations. X-ray photoelectron spectra (XPS) were collected using an ESCALAB 250 photoelectron spectrometer (ThermoFisher Scientific) with Al $K\alpha$ (1486.6 eV) as the X-ray source set at 150 W and a pass energy of 30 eV for a high-resolution scan. Raman spectra were recorded on a Lab-RAM HR Evolution (Horiba Jobin Yvon) with a 514 nm laser beam. Rheological data were collected on a TA-AR G2 rheometer by using an 8 mm diameter parallel plate with a 1 mm plate–plate gap. XRD was carried out on a D8 Advanced X-ray diffractometer with Cu $K\alpha$ radiation ($\lambda = 0.15418 \text{ nm}$, Bruker) at a scanning speed of 2° min^{-1} . SEM was recorded on a Sirion 200 field-emission scanning electron microscope. Atomic force microscopic (AFM) images were taken using a Nanoscope III MultiMode SPM (Digital Instruments). Thermogravimetric analysis (TGA) was performed using a TA-Q50 TGA under continuous flow of 40 mL min^{-1} of N_2 at a heating rate of 10 K min^{-1} . Mechanical properties of the obtained films ($5 \times 40 \text{ mm}^2$ strips) were tested on an Instron 3342 universal testing machine at a loading rate of 0.5 mm min^{-1} with a gauge length of 20 mm. Electrical conductivity was measured by a four-probe conductivity test meter (KDY-1, Kunde Technology, Co., Ltd.) at room temperature.

3. RESULTS AND DISCUSSION

3.1. Gelation of GO. GO sheets with average lateral dimensions of $17 \pm 5.0 \text{ } \mu\text{m}$ and a thickness of 0.8 nm (Figure S1) are readily dispersible into water, forming a homogeneous dispersion with a concentration of 5 mg mL^{-1} . It is believed that the repulsive hydration and electrostatic repulsion between carboxylate moieties on GO sheets are dominant over the attraction forces associated with van der Waals and hydrophobic forces, thus preventing the aggregation of GO sheets.²⁹ To reinforce the interaction between GO sheets, a water-soluble polymer, chitosan, PEI, G4NH₂, PVP, PVA, PEO, or CMC (Figure 1) was introduced into the aqueous GO

dispersion to afford additional binding interaction. It was found that the viscosity of the GO dispersion increased dramatically upon increasing the concentration of polymer. As a result, a stable GO hydrogel was formed as the polymer concentration increased to a critical value, as confirmed by the tube-inversion method (Figure 2a). This observation indicates that the addition of a polymer promotor does enhance the binding interaction between GO sheets, promoting the gelation of GO in water.²⁵ Generally, the polymer promotors listed above can be grouped into three categories according to the amounts and types of their charges: polycations (chitosan, PEI, and G4NH₂) with protonated amino groups in acidic or neutral solutions, nonionic polymers (PVP, PVA, and PEO), and polyanion (CMC). It was found that chitosan, PEI, and G4NH₂, with positively charged amino groups, are more effective gel promotors than the nonionic polymers and polyanion with critical gel concentrations (CGCs) as low as 1 wt % relative to GO. These values are much lower than those of PVP, PVA, PEO, and CMC (10–15 wt %), signifying that electrostatic attraction is more effective than hydrogen bonding for promoting GO gelation, consistent with results reported previously.^{26,27}

To give an intuitive image of GO dispersion and GO composite hydrogels in the sol and gel phases, SEM images of the lyophilized GO dispersion and the GO composite hydrogels were collected. As shown in Figure 2a, the lyophilized sample of 5 mg mL^{-1} GO dispersion keeps the original volume of its solution precursor with a 3D GO interconnected network (Figure 2b), implying that dynamic GO networks already existed in the 5 mg mL^{-1} GO dispersion.^{26,27} All the lyophilized GO/polymer composite hydrogels exhibit similar 3D GO networks with pore diameters ranging from submicrometer to several micrometers (Figure 2b), reflecting the fact that the polymer promotors did not have distinct influences on the interior microstructures of GO hydrogels and the conformation of GO sheets.

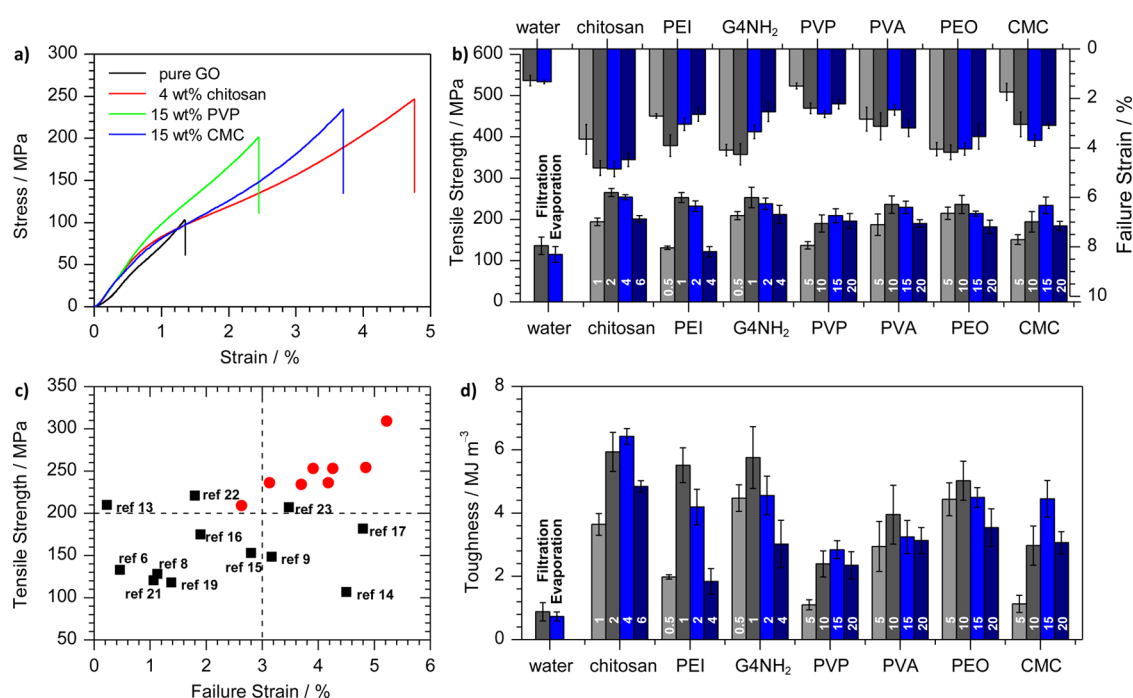


Figure 4. (a) Typical stress–strain curves of pure GO and nacre-like GO films prepared by evaporation of GO dispersion and the GFT method. (b) Ultimate strengths and failure strains of the pure GO and nacre-like GO films with different amounts of polymers as indicated. The numbers labeling the columns in the figure represent the weight ratio of the polymer to GO sheets (wt %). (c) Comparison of the ultimate strengths and failure strains of nacre-like GO films by different approaches. The scattered black points are taken from references as noted, and the red ones are nacre-like films containing the optimized amounts of polymers in this work. (d) Toughness of the GO and nacre-like GO films with different amounts of polymers as indicated (wt %).

To further clarify GO gelation process, taking chitosan and PVA for examples, small deformation oscillatory measurements were performed to monitor the storage (G') and loss (G'') moduli changes of GO dispersions upon the addition of increasing amounts of polymer promoters. In the absence of polymer, 5 mg mL⁻¹ aqueous GO dispersion gives a G' value below 0.2 kPa, with no crossover point of G' and G'' values over the entire range of tested frequencies (1–100 rad s⁻¹, Figure 2c), indicating that a loose GO network already existed in the 5 mg mL⁻¹ aqueous GO dispersion as revealed by the SEM observation (Figure 2b). Upon the introduction of polymers, both G' and G'' moduli of the GO/polymer mixtures exhibit dramatic enhancements. The G' moduli are always larger than the G'' moduli over the entire range of tested frequencies (1–100 rad s⁻¹, Figure 2d,e), and the zero shear viscosities (η_0) of the solution or hydrogels decrease linearly with shear rates (Figure S2). Thus, it is reasonable to conclude that the introduction of polymer promoters does reinforce the attraction interactions between GO sheets through electrostatic and/or hydrogen bonding interactions between GO sheets and polymers, promoting the assembly of GO sheets into a reversible highly cross-linked network. Notably, because the polymer contents were nearly the same, the GO hydrogel with 4 wt % chitosan showed G' (>730 Pa) much higher than that of the hydrogel with 5 wt % PVA (<420 Pa, Figure 2d,e), suggesting that chitosan is more efficient for promoting GO gelation. This result is also consistent with the observation that excess chitosan (6 wt % relative to GO) induced GO agglomeration rather than gelation, thus resulting in the rapid decrease in the G' and G'' moduli of the mixtures (Figure 2d).

3.2. Structures of the GO Composite Films via GFT.

Soft GO/polymer hydrogels can be easily transformed into

compact films upon cast drying under ambient conditions driven by the capillary force. The obtained GO composite films can be easily peeled off from the substrates, forming free-standing films irrespective of the polymer used. The films are smooth and uniform and can be readily obtained in large-area format and processed into the desired shapes through origami and paper-cutting because of their high toughness and flexibility (Figure 3a). The thickness and size of the GO composite films can be easily modulated by controlling the amount of GO hydrogel and the size of the container. For comparison, pure GO films were also prepared by evaporation-induced self-assembly method from aqueous GO hydrosols.

Each of the XRD patterns of GO and its composite films exhibits a sharp diffraction peak, being characteristic of the formation of a long-range orderly laminated structure (Figures 3b and S3). The interlayer spacing of the pure GO film obtained by evaporation from the aqueous GO dispersion was estimated to be 0.73 nm ($2\theta = 12.1^\circ$). This value is close to those of the pure GO films reported previously.^{6,11} Upon increasing the amounts of polymers, the diffraction peaks of GO composite films gradually shift to smaller angles, signifying the broadening of their interlayer distances. The EDS mappings across the fracture surface of the GO film with 4 wt % chitosan showed the homogeneous distributions of C, N, and O elements. Accordingly, one can conclude that polymer has been homogeneously intercalated into GO interlayers without phase separation, expanding the distances between adjacent GO sheets, and that nacre-like GO films were successfully prepared by the GFT method. It is emphasized here that by increasing the amount of polymers the diffraction peaks of all nacre-like GO films in XRD patterns are gradually broadened along with shifting to small angles with respect to those of the pure GO

film prepared by evaporation from aqueous GO dispersion (Figure 3b). These observations indicate that the inherently cross-linked structure of GO sheets in the gel matrix limits the mobility of GO sheets, making it more difficult for them to adopt an energetically favorable parallel alignment relative to those in sol phase. Correspondingly, the GFT method facilitates the formation of hierarchically structured GO films with a more interlocked wrinkled texture, alleviating the orderly alignment of GO sheets within nacre-like GO films as reported previously.²³ It is also noted that upon mixing identical amount of PEO and CMC into GO films the XRD patterns of GO/PEO composite films exhibit more pronounced dependence on the polymer contents in comparison with those of GO/CMC films. We speculated that the intrinsic structure of polymers has a critical effect on the layered structure of GO films and that the relatively hydrophobic PEO chains with more contracted conformation in aqueous solution facilitates the formation of nacre-like GO films with larger interlayer spacing.

3.3. Mechanical Performances of Nacre-Like GO Films.

All nacre-like GO films are mechanically robust, as evaluated by the tensile test measurements of at least five strips for each film (Figure 4 and Table S1). Figure 4a illustrates the typical stress–strain curves of pure GO and nacre-like GO films with an optimized thickness of 10–12 μm , fabricated by different approaches (Figure S4). As shown in Figure 4b, the ultimate strength of pure GO films by filtration and evaporation from aqueous GO dispersions were tested to be 136 ± 21 and 115 ± 19 MPa with 1.28 ± 0.21 and $1.33 \pm 0.08\%$ strain, respectively, which are comparable to those documented in the literature.⁶ For the nacre-like GO films with the addition of rationally optimized amounts of polymers casted from hydrogel precursors, the ultimate strengths reach high values of 254 ± 6 MPa (with 4 wt % chitosan), 253 ± 12 MPa (with 1 wt % PEI), 241 ± 21 MPa (with 1 wt % G4NH_2), 209 ± 17 MPa (with 15 wt % PVP), 236 ± 21 MPa (with 10 wt % PVA), 236 ± 22 MPa (with 10 wt % PEO), and 234 ± 20 MPa (with 15 wt % CMC), with distinct increases in failure strains of $4.85 \pm 0.31\%$ (chitosan), $3.91 \pm 0.44\%$ (PEI), $4.03 \pm 0.40\%$ (G4NH_2), $2.63 \pm 0.14\%$ (PVP), $3.13 \pm 0.55\%$ (PVA), $4.18 \pm 0.30\%$ (PEO), and $3.70 \pm 0.24\%$ (CMC). These tensile strengths and failure strains are 1.82–2.30 and 1.98–3.62 times, respectively, those of the pure GO films produced by evaporation of aqueous GO dispersions and are higher than those of natural nacre¹ and most of nacre-like GO films (Figure 4c).^{6,8,9,13–17,19,21–23} Moreover, the volumetric toughness of nacre-like GO films with the optimized amounts of polymers, estimated by integrating the areas under the stress–strain curves, gives average values of 6.42 ± 0.25 MJ m^{-3} (chitosan), 5.51 ± 0.55 MJ m^{-3} (PEI), 5.13 ± 0.86 MJ m^{-3} (G4NH_2), 2.84 ± 0.28 MJ m^{-3} (PVP), 3.95 ± 0.93 MJ m^{-3} (PVA), 5.06 ± 0.62 MJ m^{-3} (PEO), and 4.45 ± 0.58 MJ m^{-3} (CMC; Figure 4d), which are also higher than most of the reported values for nacre-like GO films.⁴ These results indicate that GO/polymer composite hydrogels are excellent precursors for nacre-like GO films and that the GFT approach is an efficient method toward the fabrication of nacre-like GO films with excellent integration of tensile strength, failure strain, and toughness.

It is noted that all nacre-like GO films examined here achieve superior mechanical performances with high tensile strength, strain, and toughness irrespective of the intrinsic structures of the polymer promoters, including shapes (linear, branched, or superbranched), molar masses, and the types of charges. However, the polymer gel promoters with lower CGCs

(chitosan, PEI, and G4NH_2) seem to be preferred for preparing nacre-like GO films with the greatest mechanical performance because an excessive amount of polymers would result in a larger interlayer distance and consequently alleviate the interlayer interactions. The strong electrostatic interaction between GO sheets and positively charged ammonium side chains of chitosan, PEI, and G4NH_2 would be another merit for further enhancing mechanical performances of the resultant nacre-like GO films.

3.4. Effects of GFT on the Mechanical Properties of Nacre-Like GO Films. To compare GFT with other film formation methods, a GO/PEO composite film was fabricated via vacuum-assisted filtration of an aqueous GO hydrosol (1.0 mg mL^{-1}) containing 10 wt % PEO (Figure S5). The mechanical performance of the GO composite film from hydrosol was shown to be comparable to that of the pure GO film prepared through the same process and much inferior to that of the GFT-prepared nacre-like GO film containing the same amount of PEO (Figures 5a and S5b). This observation

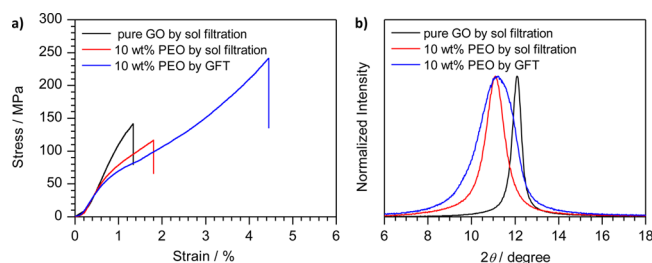


Figure 5. (a) Typical stress–strain curves and (b) XRD patterns of pure GO film by filtration and nacre-like GO films with 10 wt % PEO prepared by filtration of hydrosol (1 mg mL^{-1} GO) and GFT method (5 mg mL^{-1} GO).

reflects the fact that GFT technique is much better than vacuum-assisted filtration for fabricating GO films with high mechanical properties. This phenomenon can be explained by the microstructural difference of the GO films prepared through both approaches. The GO composite film prepared from GO hydrosol with the same amount of PEO exhibited a XRD diffraction peak narrower than that of the GFT-directed GO film (Figure 5b). Accordingly, the hydrosol processing method facilitates the assembly of GO sheets into highly short-range-ordered film with energetically favorable parallel alignment because of their high freedom of motion in the sol phase. It is known that the sp^3 defects together with their intrinsic flexibility enable GO sheets to have a wrinkled topology at the nanoscale in aqueous dispersion.²⁹ During GFT, the limited mobility of GO sheets in the gel matrix because of the presence of physical cross-linking points between GO sheets induces a more wrinkled texture within GO basal plane, accounting for the less ordered alignment of GO sheets in the film with a broadened XRD diffraction peak (Figure 5b).²³ The wrinkled texture is favorable for intimate interaction and better adhesion between the adjacent GO sheets and consequently induces the formation of a mechanically interlocked structure through the wrinkles. The wrinkled structures may also afford an additional mechanical interlocking between GO sheets and polymer chains. Taken together, one may conclude that the hierarchical structures with the highly interlocked wrinkles in GFT films are favorable for stress transfer and strain enlargement and are coupled directly to the distinct mechanical performance.^{23,30}

3.5. Effects of GO Structures on the Properties of Nacre-Like GO Films. It has been reported that the size of GO sheets has a strong influence on the mechanical properties of the GO films.¹¹ To address the influence of this factor on the mechanical performance of GFT-directed nacre-like GO films, larger GO sheets with mean lateral dimensions of $26 \pm 10 \mu\text{m}$ (denoted as GO' hereafter) were prepared via a modified synthesis approach by decreasing the oxidation temperature from 40 to 30 °C (Figure S6). Taking chitosan as an example, nacre-like GO' films (Figure S7) were prepared by the GFT method, and their mechanical performances were evaluated (Table S1). The rationally optimized nacre-like GO film containing 4 wt % chitosan exhibited dramatic enhancement in both tensile strength and failure strain, giving a maximum tensile strength of $309 \pm 21 \text{ MPa}$ with a failure strain of 5.22 ± 0.43 (Figure 6). The volumetric toughness derived from the

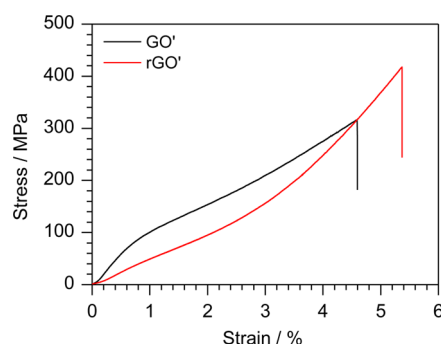


Figure 6. Typical stress–strain curves of nacre-like GO' film with 4 wt % chitosan and the corresponding reduced GO' film prepared by the GFT method.

stress–strain curves was calculated to be as high as $8.26 \pm 0.68 \text{ MJ m}^{-3}$. To our knowledge, these values are the highest among those reported for nacre-like GO films.⁴

Nacre-like GO films are nearly insulating because of the presence of abundant oxygen-containing groups on both sides of the GO basal planes, which disrupts the conjugation structure and introduces lattice defects. Chemical reduction of GO can remove most of oxygenated moieties on the GO basal plane, resulting in the restoration of its conjugated network and conductivity. To expand the properties of nacre-like GO films beyond mechanical performance, the GO film containing 4 wt % chitosan was submitted to chemical reduction with HI aqueous solution. The reduced GO' film achieves high electrical conductivity of $374 \pm 6 \text{ S cm}^{-1}$ as well as improved mechanical performance, with a tensile strength of $424 \pm 22 \text{ MPa}$, a failure strain of $5.52 \pm 0.39\%$, and a volumetric toughness of $8.98 \pm 0.73 \text{ MJ m}^{-3}$. These results indicate that the GFT method has great potential in the fabrication of high-performance, multifunctional, nacre-like graphene structural materials.

4. CONCLUSIONS

GFT is a general and facile method to prepare nacre-like GO films with superior mechanical performance. This method can be readily scaled-up for mass-production of robust nacre-like GO films with different compositions because most commercially available water-soluble polymers can be used as gel promoters to induce GO gelation. Furthermore, GO sheets can be readily produced by cost-effective wet chemical approaches, having good compatibility with traditional techniques for

operation and scalability for industrial utilization. We believe that the present work will not only provide a convenient method for preparing robust nacre-like GO films but also promote the application exploration of these films in different areas.

■ ASSOCIATED CONTENT

● Supporting Information

XPS patterns; Raman spectra; AFM and SEM images of GO and GO' sheets; viscosities at different shear rates and zero-shear viscosities (η_0) of GO and GO/polymer mixtures with different amounts of chitosan and PVA; XRD patterns of GO composite films with different amounts of G4NH₂, PVP, and PVA; thickness-dependent mechanical performances of GO films containing 4 wt % chitosan; photographs of 1 and 5 mg mL⁻¹ GO dispersions containing 10 wt % PEO relative to GO; TGA curves of pure GO and GO composite films containing 10 wt % PEO; and XRD patterns of GO' composite films with different amount of chitosan. The Supporting Information is available free of charge on the ACS Publications website at DOI: 10.1021/acsami.5b04093.

■ AUTHOR INFORMATION

Corresponding Authors

*E-mail: chunli@mail.tsinghua.edu.cn.

*E-mail: syunano@imu.edu.cn.

*E-mail: gshi@tsinghua.edu.cn.

Notes

The authors declare no competing financial interest.

■ ACKNOWLEDGMENTS

This work was supported by the National Basic Research Program of China (2012CB933402) and the Natural Science Foundation of China (21274074, 51433005).

■ REFERENCES

- (1) Espinosa, H. D.; Rim, J. E.; Barthelat, F.; Buehler, M. J. Merger of Structure and Material in Nacre and Bone-Perspectives on De Novo Biomimetic Materials. *Prog. Mater. Sci.* **2009**, *54*, 1059–1100.
- (2) Meyers, M. A.; McKittrick, J.; Chen, P.-Y. Structural Biological Materials: Critical Mechanics-Materials Connections. *Science* **2013**, *339*, 773–779.
- (3) Yao, H.-B.; Ge, J.; Mao, L.-B.; Yan, Y.-X.; Yu, S.-H. 25th Anniversary Article: Artificial Carbonate Nanocrystals and Layered Structural Nanocomposites Inspired by Nacre: Synthesis, Fabrication and Applications. *Adv. Mater.* **2014**, *26*, 163–188.
- (4) Cheng, Q.; Jiang, L.; Tang, Z. Bioinspired Layered Materials with Superior Mechanical Performance. *Acc. Chem. Res.* **2014**, *47*, 1256–1266.
- (5) Wegst, U. G. K.; Bai, H.; Saiz, E.; Tomsia, A. P.; Ritchie, R. O. Bioinspired Structural Materials. *Nat. Mater.* **2014**, *14*, 23–36.
- (6) Dikin, D. A.; Stankovich, S.; Zimney, E. J.; Piner, R. D.; Dommett, G. H. B.; Evmenenko, G.; Nguyen, S. T.; Ruoff, R. S. Preparation and Characterization of Graphene Oxide Paper. *Nature* **2007**, *448*, 457–460.
- (7) Chen, H.; Müller, M.; Gilmore, K. J.; Wallace, G. G.; Li, D. Mechanically Strong, Electrically Conductive, and Biocompatible Graphene Paper. *Adv. Mater.* **2008**, *20*, 3557–3561.
- (8) Satti, A.; Larpent, P.; Gun'ko, Y. Improvement of Mechanical Properties of Graphene Oxide/Poly(Allylamine) Composites by Chemical Crosslinking. *Carbon* **2010**, *48*, 3376–3381.
- (9) Putz, K. W.; Compton, O. C.; Palmeri, M. J.; Nguyen, S. T.; Brinson, L. C. High-Nanofiller-Content Graphene Oxide-Polymer Nanocomposites via Vacuum-Assisted Self-Assembly. *Adv. Funct. Mater.* **2010**, *20*, 3322–3329.

- (10) Putz, K. W.; Compton, O. C.; Segar, C.; An, Z.; Nguyen, S. T.; Brinson, L. C. Evolution of Order during Vacuum-Assisted Self-Assembly of Graphene Paper and Associated Polymer Nanocomposites. *ACS Nano* **2011**, *5*, 6601–6609.
- (11) Lin, X.; Shen, X.; Zheng, Q.; Yousefi, N.; Ye, L.; Mai, Y.-W.; Kim, J.-K. Fabrication of Highly-Aligned, Conductive, and Strong Graphene Oxide Papers Using Ultralarge Graphene Oxide Sheets. *ACS Nano* **2012**, *6*, 10708–10719.
- (12) Zhu, J.; Zhang, H.; Kotov, N. A. Thermodynamic and Structural Insights into Nanocomposites Engineering by Comparing Two Materials Assembly Techniques for Graphene. *ACS Nano* **2013**, *7*, 4818–4829.
- (13) Tian, Y.; Cao, Y.; Wang, Y.; Yang, W.; Feng, J. Realizing Ultrahigh Modulus and High Strength of Macroscopic Graphene Oxide Papers through Crosslinking of Mussel-Inspired Polymers. *Adv. Mater.* **2013**, *25*, 2980–2983.
- (14) Cheng, Q.; Wu, M.; Li, M.; Jiang, L.; Tang, Z. Ultratough Artificial Nacre Based on Conjugated Cross-Linked Graphene Oxide. *Angew. Chem., Int. Ed.* **2013**, *52*, 3750–3755.
- (15) Hu, K.; Tolentino, L. S.; Kulkarni, D. D.; Ye, C.; Kumar, S.; Tsukruk, V. V. Written-in Conductive Patterns on Robust Graphene Oxide Biopaper by Electrochemical Microstamping. *Angew. Chem., Int. Ed.* **2013**, *52*, 13784–13788.
- (16) Cui, W.; Li, M.; Liu, J.; Wang, B.; Zhang, C.; Jiang, L.; Cheng, Q. A Strong Integrated Strength and Toughness Artificial Nacre Based on Dopamine Cross-Linked Graphene Oxide. *ACS Nano* **2014**, *8*, 9511–9517.
- (17) Wan, S.; Li, Y.; Peng, J.; Hu, H.; Cheng, Q.; Jiang, L. Synergistic Toughening of Graphene Oxide-Molybdenum Disulfide-Thermoplastic Polyurethane Ternary Artificial Nacre. *ACS Nano* **2015**, *9*, 708–714.
- (18) Lee, D. W.; Hong, T.-K.; Kang, D.; Lee, J.; Heo, M.; Kim, J. Y.; Kim, B.-S.; Shin, H. S. Highly Controllable Transparent and Conducting Thin Films Using Layer-by-Layer Assembly of Oppositely Charged Reduced Graphene Oxides. *J. Mater. Chem.* **2011**, *21*, 3438–3442.
- (19) Li, Y.-Q.; Yu, T.; Yang, T.-Y.; Zheng, L.-X.; Liao, K. Bio-Inspired Nacre-like Composite Films Based on Graphene with Superior Mechanical, Electrical, and Biocompatible Properties. *Adv. Mater.* **2012**, *24*, 3426–3431.
- (20) Xin, G.; Sun, H.; Hu, T.; Fard, H. R.; Sun, X.; Koratkar, N.; Borca-Tasciuc, T.; Lian, J. Large-Area Freestanding Graphene Paper for Superior Thermal Management. *Adv. Mater.* **2014**, *26*, 4521–4526.
- (21) Liu, Z.; Li, Z.; Xu, Z.; Xia, Z.; Hu, X.; Kou, L.; Peng, L.; Wei, Y.; Gao, C. Wet-Spun Continuous Graphene Films. *Chem. Mater.* **2014**, *26*, 6786–6795.
- (22) Huang, L.; Li, C.; Yuan, W.; Shi, G. Strong Composite Films with Layered Structures Prepared by Casting Silk Fibroin-Graphene Oxide Hydrogels. *Nanoscale* **2013**, *5*, 3780–3786.
- (23) Zhang, M.; Huang, L.; Chen, J.; Li, C.; Shi, G. Ultratough, Ultrastrong, and Highly Conductive Graphene Films with Arbitrary Sizes. *Adv. Mater.* **2014**, *26*, 7588–7592.
- (24) Ouyang, W.; Sun, J.; Memon, J.; Wang, C.; Geng, J.; Huang, Y. Scalable Preparation of Three-Dimensional Porous Structures of Reduced Graphene Oxide/Cellulose Composites and Their Application in Supercapacitors. *Carbon* **2013**, *62*, 501–509.
- (25) Li, C.; Shi, G. Functional Gels Based on Chemically Modified Graphenes. *Adv. Mater.* **2014**, *26*, 3992–4012.
- (26) Bai, H.; Li, C.; Wang, X.; Shi, G. On the Gelation of Graphene Oxide. *J. Phys. Chem. C* **2011**, *115*, 5545–5551.
- (27) Bai, H.; Li, C.; Wang, X.; Shi, G. A pH-Sensitive Graphene Oxide Composite Hydrogel. *Chem. Commun.* **2010**, *46*, 2376–2378.
- (28) Zhang, M.; Yuan, W.; Yao, B.; Li, C.; Shi, G. Solution-Processed PEDOT:PSS/Graphene Composites as the Electrocatalyst for Oxygen Reduction Reaction. *ACS Appl. Mater. Interfaces* **2014**, *6*, 3587–3593.
- (29) Cheng, C.; Li, D. Solvated Graphenes: An Emerging Class of Functional Soft Materials. *Adv. Mater.* **2013**, *25*, 13–30.
- (30) Jalili, R.; Aboutalebi, S. H.; Esrafilzadeh, D.; Konstantinov, K.; Moulton, S. E.; Razal, J. M.; Wallace, G. G. Organic Solvent-Based Graphene Oxide Liquid Crystals: A Facile Route toward the Next Generation of Self-Assembled Layer-by-Layer Multifunctional 3D Architectures. *ACS Nano* **2013**, *7*, 3981–3990.